CHAPTER III

The Particle Size Reduction of Beclomethasone Dipropionate Monohydrate by Thermal Dehydration: Dehydration Energy, Apparent Particle Size Reduction Energy and Controlled Mechanism

3.1 INTRODUCTION

Beclomethasone dipropionate monohydrate (BDM) was chosen as a model compound for the particle size reduction via thermal dehydration determined from previous reports (Narueporn Nachiengtung, 1997 and Amolwan Chinapak, 2001). The dehydration of BDM which eventually resulted in smaller particle size of anhydrous beclomethasone dipropionate (BD) was initially discovered by Narueporn Nachiengtung (1997). During an attempt to investigate BDM polymorphic transformation of in aerosol suspension, they reported the particle size reduction event of BDM to BD while crystallize water was removed by vacuum or temperature drying. This phenomenon was further studies by Amolwan Chinapak (2001). They found that the higher the dehydration energy, the faster the size reduction while the final particle size was similarly distributed.

The aim of this study was to evaluate the mechanism which controlled the particle size reduction by thermal dehydration of BDM. The quantification of energy either for dehydration or apparently reduce particle size at different temperatures was determined.

3.2 EXPERIMENT

3.2.1 CHEMICALS

- Beclomethasone dipropionate anhydrous (Lot No. 7849/M1, Sicor, Italy)
- Double distilled water
- Absolute ethanol (Merck, Germany)
- Polyoxyethylene sorbitan monooleate (supplied by Srichand United Dispensary, Thailand)

3.2.2 INSTRUMENTS

- Differential Scanning Calorimeter (822^e, Mettler Toledo, Switzerland)
- Thermogravimetric Analyzer (TGA/SDTA851^e, Mettler Toledo, Switzerland)
- Hot stage (FP90, Mettler Toledo, Switzerland) equipped with optical microscope (Eclipse E2000, Nikon, Japan)
- Standard sieve analyzer (FT-150M, Filtra vibraciòn, Spain)
    - Sieve mesh No 40 (equivalent to 425 micron)
    - Sieve mesh No 100 (equivalent to 150 micron)
- X-ray Powder Diffractometer (D5000, Siemens, Germany)
- Scanning Electron Microscope (JSM-5410 LV, Jeol, Japan)
- Laser diffraction particle size analyzer (Mastersizer S, Malvern, UK)

3.2.3 METHODS

Preparation of Monohydrate Form of Beclomethasone Dipropionate

Antisolvent recrystallization was employed to produce BDM. Due to its hydrophobicity, BD was dissolved in ethanol whereas water was selected as antisolvent. Directly dissolve 0.75 g of BD into 35 ml of absolute ethanol in a well closed system at ambient condition. Clear and colorless solution was developed with continuous mixing. Fifty millilitres of double distilled water was gradually added into BD ethanolic solution with continuous stirring. The rate of water addition was 4 ml/min. Small and clear crystals of BDM were generated. The BDM crystal was harvested and further air dried at ambient condition. Selection of particle size was done by sieve analyzer. Crystal size within the range of 150 to 425 microns (328 microns) was retained for future dehydration experiment.

Solid State Characterization

Solid state characterization of BDM generated, dehydrated BDM and initial BD were performed by thermal analysis and X-ray Powder Diffraction (XRPD).

Crystal morphology

Crystal morphology of each solid was investigated by Scanning electron microscope (SEM). The sample was carefully dispersed and attached on the metal stub. It was then sputter coated with gold before its morphology was recorded. The degree of magnification of the instrument was varied depending on the nature of the sample.

Thermal analysis

Evaluation of the thermal properties of the solids was determined by DSC in conjunction with STAR^e software for data processing. The sample weight of approximately 5 to 10 mg was placed in standard aluminum pan (40 µl) and sealed with pierced lid. The scanning rate was 10 °C/min and the temperature range was 30 to 230 °C. Dried nitrogen gas at the rate of 60 ml/min was purged throughout the study to avoid oxidative decomposition upon heat treatment. DSC Calibration using standard indium was periodically done.

In order to confirm the monohydrate stoichimomtery of BDM produced, weight loss of sample was analyzed using TGA. The sample container, heating

condition and software were the same as that used in DSC. The experiment was done in triplicate. Net change in mass was calculated to reveal the stoichiometry of water of crystallization.

Hot stage microscope (HSM) was employed to show the existence of hydrate. Small amount of sample was dispersed in mineral oil and placed on the glass slide on the top of the hot stage microscope using the scanning rate of 10 °C/min. The evolution of water vapor bubbles was observed and recorded. In addition, preliminary observation on the particle size reduction phenomena during heating was also performed and recorded by HSM.

XRPD

Identification of the molecular arrangement of the solid samples were determined via XRPD. Wide angle XRPD using CuKα generator at 40kV and 20mA was employed. The scan speed, scan step and angular scan range was set at 5° per min, 0.04° per step and 5 to 35 ° 2θ, respectively.

Thermally Assisted Particle Size Reduction of BDM

Thermal dehydration under isothermal mode of DSC (IDSC) was chosen to investigate the particle size reduction and dehydration phenomena (Brown, Galwey and Po, 1993). According to preliminary study, the crystal size of BDM was reduced at elevated temperature as water molecules were removed. Thus, quantification of energy utilized during dehydration was collected. The total energy consumption (Joule per second) over time (second) at each temperature obtained from IDSC was recorded and calculated as energy of reaction. On the other hand, samples were periodically collected during the experiment and the remaining water was also determined by TGA.

BDM with the average size between 150 to 425 microns was accurately weighed (12 mg) and placed in standard 40 µl aluminum pan without cover. It was positioned on the DSC furnace with the other reference aluminum pan. Dried nitrogen gas was purged over the sample at 60 ml/min. The change in power consumption as a function of heating time was recorded. The isothermal temperatures (T_{iso}) were fixed at 55, 60, 65 and 70 °C. Furthermore, samples were collected periodically during various dehydration stages of IDSC to monitor for the particle size and the remaining amount of water.

The particle size of thermally treated BDM was investigated by laser diffraction particle size analyzer. Water was the dispersion medium since it would not dissolved BDM. Due to low wettability of the sample, 1% w/v Polyoxyethylene sorbitan monooleate was needed to readily disperse BDM in aqueous medium. Particle size determination was carried out in triplicate and the average value of mean particle diameter (d [v,0.5]) was obtained. Water content in the samples was determined by TGA.

The energy consumption-dehydration time profile obtained from IDSC could be used to calculate the energy of reaction (Kishore, 1978). Area under the curve (AUC) of IDSC is directly proportional to the total energy of reaction. In this experiment, trapezoidal rule was applied to determine the energy of reaction.

The relationship among reaction energy, particle size and water content were established.

Determination of Dehydration Activation Energy (E_a) of BDM

Model dependent solid state kinetic (Byrn et al., 1999)

The E_a of dehydration can be calculated along with the Arrhenius assumption. The relationship between the fraction reacted (α) and the reaction time (t) were collected. The α value can be defined as

$$\alpha = \frac{AUC_{0\to t}}{AUC_{0\to\infty}} \qquad \ldots(17)$$

Where $AUC_{0\text{-}t}$ is area under IDSC curve from time zero to any time (t) and $AUC_{0\text{-}\infty}$ is area under IDSC curve from time zero to infinite time (t_∞) (Khawam and Flanagan, 2006).

After the relationship between α and t was constructed, the α of 0.2 to 0.8 which theoretically gives a straight line was selected. The data in this region were fitted with defined solid state kinetic model equations. The constant (k) from each model was determined. Best fitted models were chosen from the highest correlation of determination (r^2), generally greater than 0.99.

According to the Arrhenius equation, k is related to temperature and E_a can be calculated as follow

$$k = Ae^{-\frac{E_a}{RT}} \qquad \ldots(18)$$

by taking natural logarithm (ln),

$$\ln k = \ln A - \frac{E_a}{R} \cdot \frac{1}{T} \qquad \ldots(19)$$

where k is the rate constant, A is a pre-exponential factor or frequency factor, R is the gas constant and T is the absolute temperature in Kelvin.

Therefore, a plot of ln k from the solid state kinetic model versus reciprocal absolute temperature (1/T) will give E_a of dehydration from the slope ($-E_a/R$) value.

Model independent solid state kinetic

In an attempt to find the robust method for E_a calculation, model independent or model free method of solid state kinetic were developed (Khawam and Flanagan, 2005 and 2006). Model dependent kinetic approach is actually based on certain mechanistic assumptions; and the most important assumption is that the reaction must be a homogeneous reaction. Thus, it is not versatile enough to apply to all reaction kinetic. Meanwhile, the independent model does not have an assumption like model dependent. By this model independent kinetic approach, it will provide E_a as a function of α.

In a model independent approach, isoconversion method was introduced. Derivation of the integrated function of the rate equation from isoconversion method is presented in Appendix B. From integral reaction model $g(\alpha)$

$$g(\alpha) = Ae^{-\frac{E_a}{RT}}t \qquad \ldots(20)$$

by taking natural logarithm

$$\ln g(\alpha) = \ln A - \frac{E_a}{RT} + \ln t \qquad \ldots(21)$$

which can be rearranged to

$$\ln t = \frac{E_a}{R} \cdot \frac{1}{T} - \ln\left(\frac{A}{g(\alpha)}\right) \qquad \ldots(22)$$

There are a few methods (standard isoconversion method and Friedman's isoconversion method) introduced and used for E_a determination. In this experiment, standard method was selected. A plot between α and t (at each temperature level), similar to model dependent approach, was done. At each α value, t value was determined for different temperatures. The ln t was plot with respect to 1/T. The slope from linear relationship of ln t and 1/T was calculated and resolved as E_a.

3.3 RESULTS AND DISCUSSION

Characterization of BDM Produced

The results from thermal analysis and XRPD analysis of BDM are shown in Figure 3.1 and Figure 3.7, respectively.

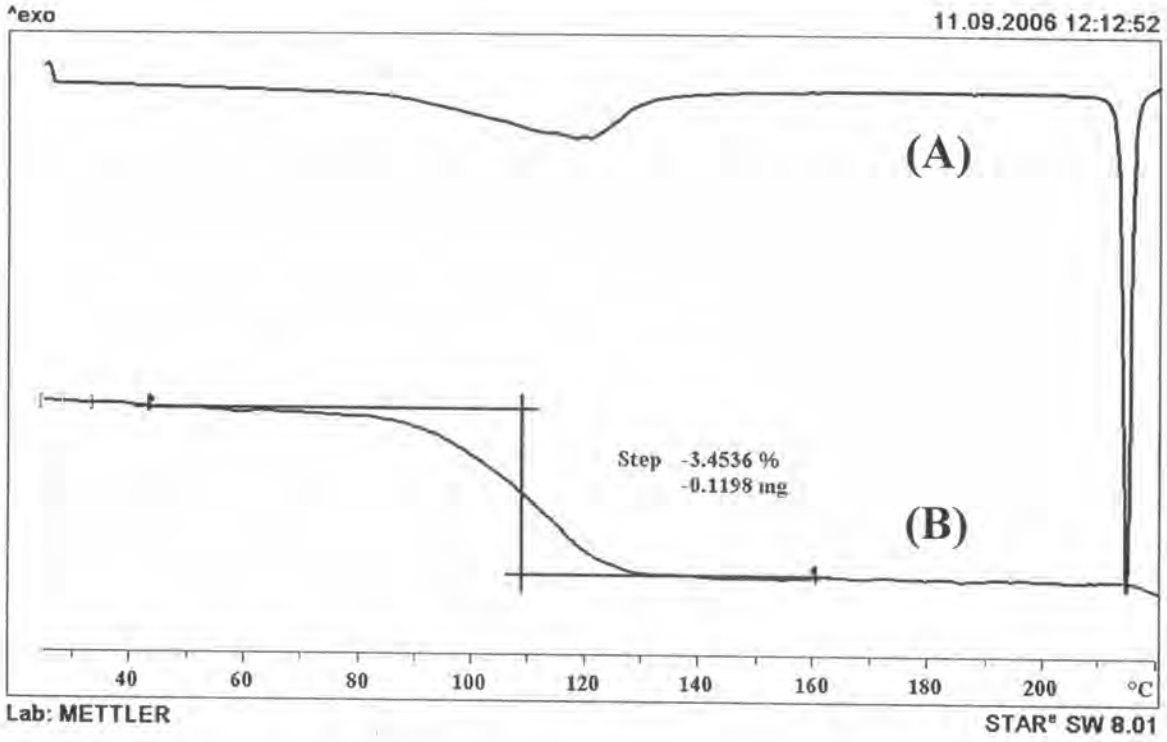

Figure 3.1 Thermograms of BDM according to (A) DSC and (B) TGA, at a scanning rate of 10 °C/min

Thermal behavior of BDM produced showed typical pattern of a stoichiometric hydrate which consisted of a large and broad DSC endotherm at low temperature (70 to 130 °C) in conjunction with weight loss seen in TGA during the same temperature range. The sharp DSC endothermic peak with the onset temperature of approximately 214 °C was present without any change in mass indicating the melting endotherm after water of crystallization in BDM was removed. The weight loss of BDM was 3.4 %w/w and correlated with the theoretical stoichiometric monohydrate of 3.34 %w/w. To confirm the correct hydrate stoichiometry, water content must be quantified by Karl Fischer (KF) titrimetry and compared to the weight loss obtained by TGA. In this case, BDM has a ketone functional group and

will provide an overestimation of the water content from side reaction of KF and special reagents are recommended (Narueporn Nachiengtung, 1997). Therefore, KF was not selected in this study. XRPD was chosen to identify the monohydrate structure of the produced BDM instead. From XRPD pattern of the solid, the peak position at different degrees 2θ was identical to BDM obtained and characterized by Narueporn Nachiengtung (1997) and was used as reference. In addition, HSM was also performed to investigate the hydrated state of BDM produced. The result showed the evolution of vapor bubbles during heating at 70 to 130 °C (Figure 3.3). From the above evidence, the solid powder produced is characterized and identified as BD with monohydrate stoichiometry.

The physical appearance of BDM was recorded by SEM (Figure 3.2). It was tabular in shape and had a wide particle size distribution. In order to prepare a suitable particle size of BDM for dehydration experiments, sieve analysis was done by using sieve mesh No. 40 and No. 100. Selected BDM sample retained between sieve No. 40 and No. 100 had mean particle diameter (d[v,0.5]) of approximately 328 microns as determined with laser particle size analyzer.

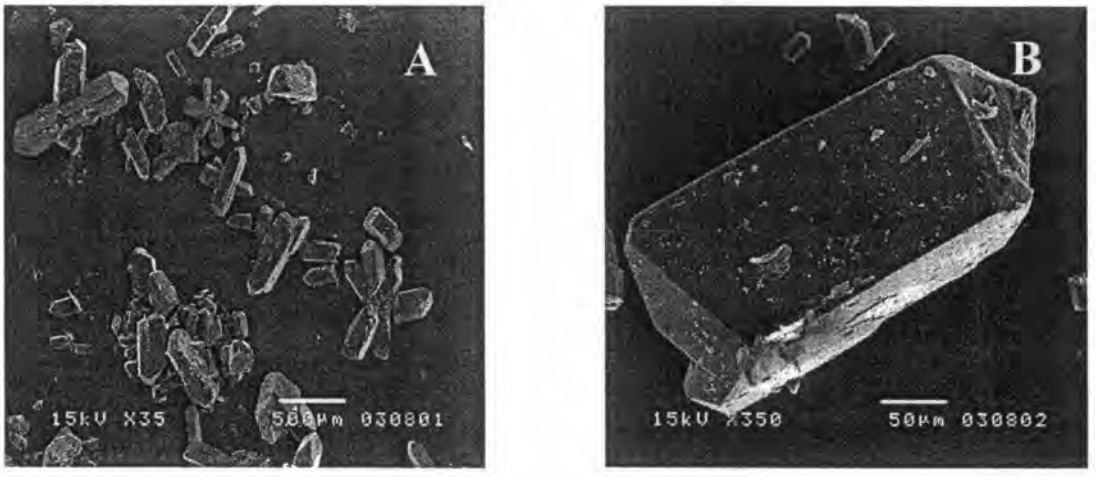

Figure 3.2 Scanning electron photomicrographs of BDM crystals (A-magnification of 35 and B-magnification of 350)

A preliminary study to show possibility on particle size reduction of BDM by dehydration was carried out by HSM. As a function of heating temperature, BDM crystal showed dehydration sign at early stage seen with vapor bubbles liberated (Figure 3.3). In addition, the defect around outer surface of BDM crystal took place

and occurred continuously with respect to temperature. A disruption of crystal was seen as an opaque region on the outer surface of the crystal. Defects of BDM crystals were gradually expanding in area and eventually resulted in fragmented crystals of opaque BD. The crystallographic transformation of BDM to BD during dehydration was also investigated with XRPD. The results revealed that BDM gradually changed to BD as can be seen in Figure 3.7.

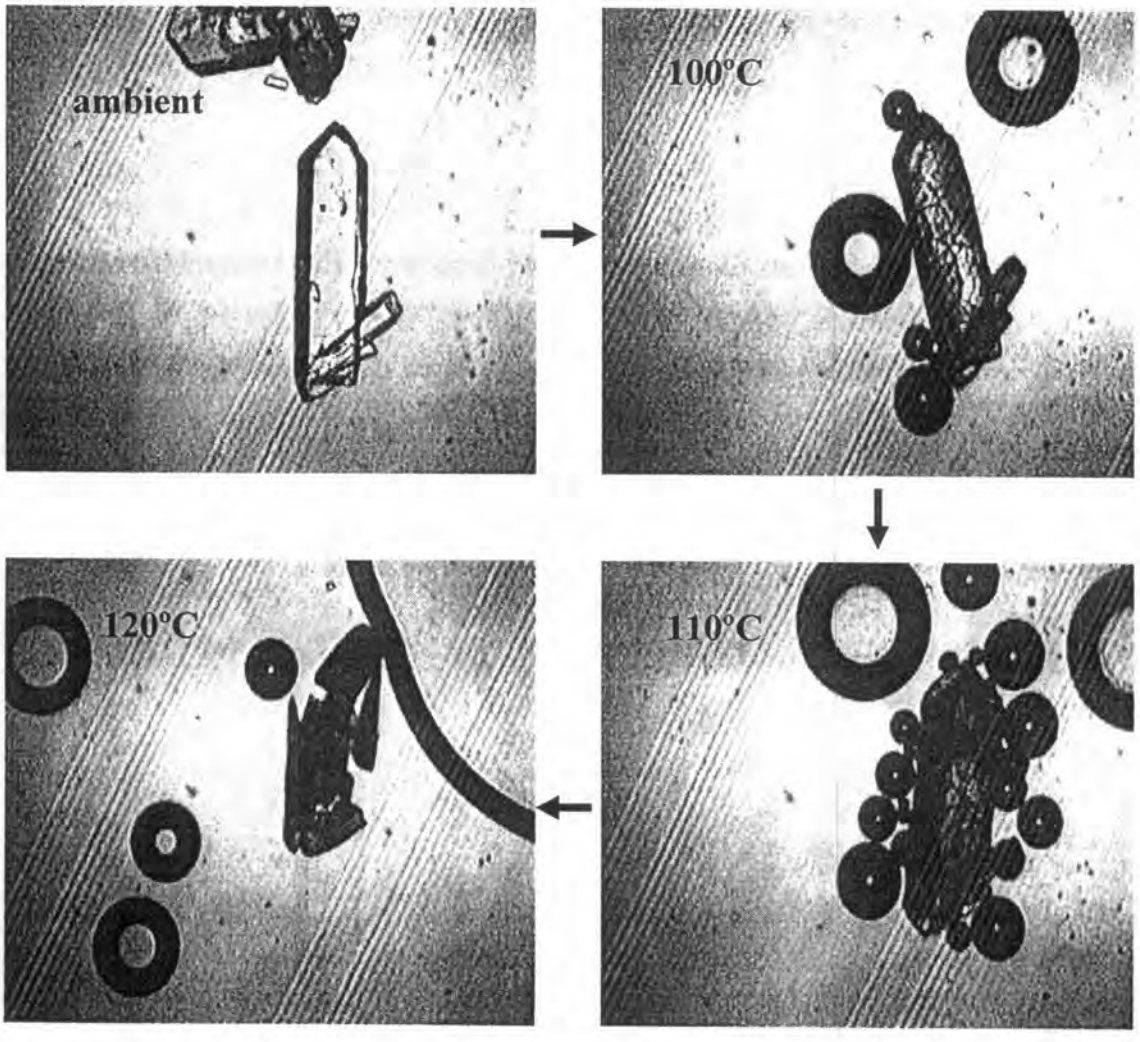

Figure 3.3 Photomicrographs of BDM immersed in mineral oil during heating under hot stage microscope at the rate of 10 °C/min

Dehydration and particle size reduction of BDM

There are previous reports showing the particle size of BDM may be reduced during heating to its anhydrous state (Narueporn Nachiengtung, 1997 and Amolwan Chinapak, 2000). One of the most important parameter to consider during thermal dehydration was the energy involved. The energy of reaction can be quantified by

using DSC isothermal mode of heating and indirectly determining the energy consumed during dehydration of BDM. Due to a constant temperature used in an isothermal heating method, the progress of dehydration stages of BDM was monitored as a function of heating time.

The results of isothermal dehydration of BDM at different isothermal temperatures (T_{iso}) are shown in Figure 3.4. The IDSC thermograms composed of one large endotherm. The early stage of reaction showed the large and broad endotherm which directly implied to the energy consumed during dehydration of BDM. The later stage exhibited a constant power level indicating that there was no energy needed for later stages. Moreover, the remaining water content of BDM at later stage of IDSC was less than 0.5 % w/w (Figure 3.6) and confirmed complete BDM dehydration immediately after the observed large endotherm.

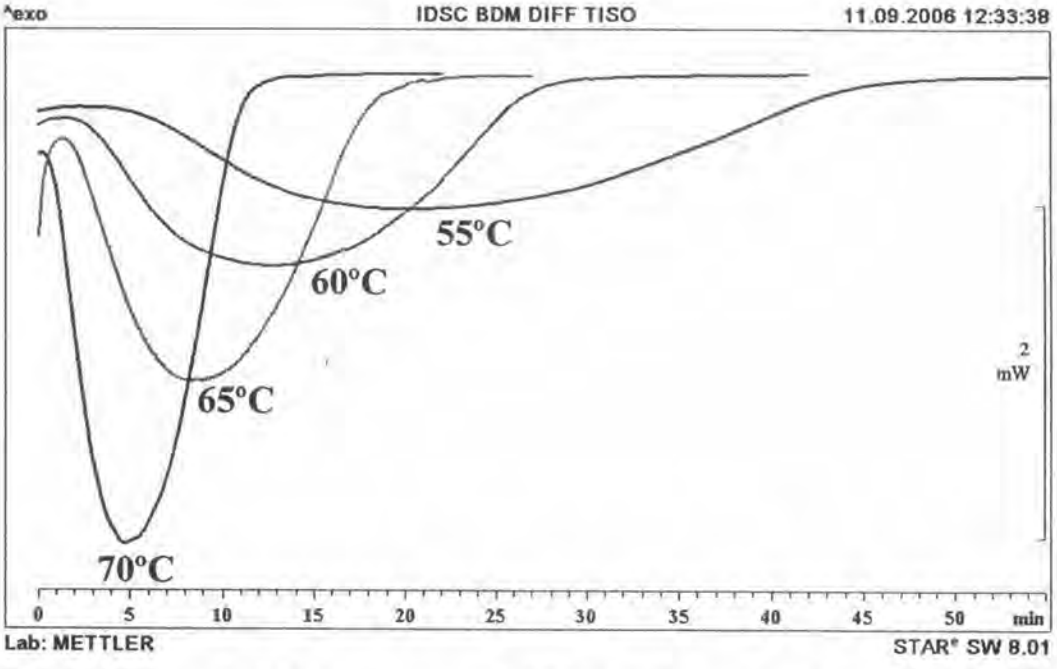

Figure 3.4 Isothermal DSC thermograms of BDM with respect to various T_{iso}

The AUC of obtained endotherm from IDSC at each T_{iso} were calculated and defined as the dehydration energies and are illustrated in Table 3.1. In addition, the enthalpy of dehydration obtained with non-isothermal DSC (NIDSC) method of BDM was used for comparison with IDSC method and was found to be 88.93 ± 0.30 J/g. The dehydration energies from NIDSC and IDSC methods were consistent and indicated the suitability of IDSC method for quantitative determination of dehydration

energy on the temperature dependency. The total energy for dehydration of BDM at every T_{iso} found not to be statistically different. The different T_{iso} did not have any influence on total energy of dehydration. It could be said that the total dehydration energy of BDM did not depend on temperature within the specified range of 55 to 70 °C.

Table 3.1 The apparent particle size reduction energy and the total dehydration energy used for complete dehydration of BDM at different T_{iso}

T_{iso} (°C)	Apparent particle size reduction energy (J/g)	Total dehydration energy (J/g)
55	29.23 ± 0.76	79.74 ± 0.30
60	24.04 ± 0.51	80.85 ± 2.02
65	17.83 ± 1.48	78.35 ± 1.70
70	48.57 ± 1.25	78.37 ± 3.94

As described earlier, the particle size of BDM was reduced during the dehydration process. The particle size of BDM during IDSC was monitored with respect to T_{iso} and the energy used (Figure 3.5). In addition, the remaining water content of isothermally heated BDM was investigated and is shown in Figure 3.6. The particle size of BDM dramatically reduced to a lower size at initial stage of dehydration phase. The apparent time which resulted in the smallest particle size were observed at the peak of IDSC thermograms at every T_{iso} where the slope was zero (Figure 3.4). Thus, at every T_{iso} used, the required energy to produce the lowest particle size of BD was obtained from AUC calculated since the beginning until peak of IDSC thermograms and will be defined as the apparent particle size reduction energy. The result suggested that the apparent particle size reduction energy was lower than total required energy for dehydration comparing Figure 3.5, Figure 3.6 and Table 3.1. One must keep in mind that although thermal dehydration could effectively reduce the particle size of BDM to lowest possible but this still resulted in a mixture between BD and BDM solid structures when inappropriate amount of energy was applied. The optimal energy needed to yield a pure phase BD with smallest particle size should be determined in the future.

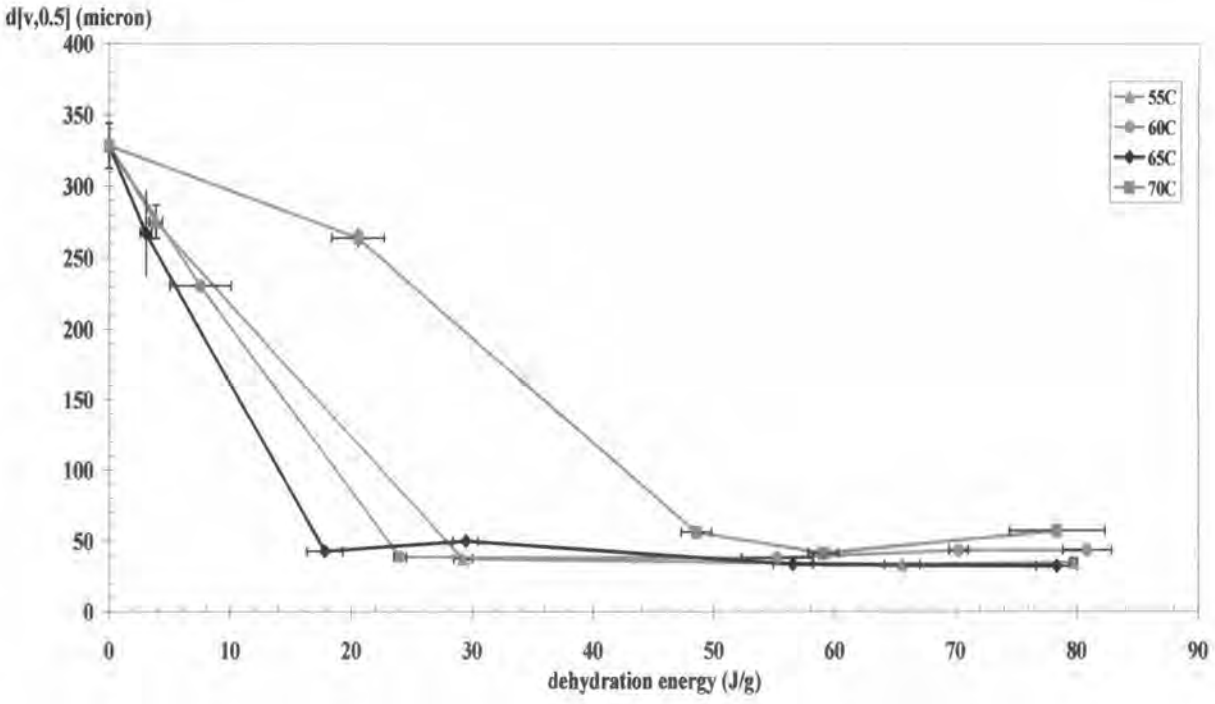

Figure 3.5 The relationship between mean particle diameter d[v,0.5] and the dehydration energy when BDM was isothermally heated (T_{iso}) at ▲ 55°C, ● 60°C, ◆ 65°C and ■ 70°C

From Figure 3.5, the temperatures of 55, 60, 65 °C, the particle size of BDM reduced at initial stage of isothermal dehydration and did not change further at the later stage. The minimal size was 30 to 60 microns and was significantly different from intact BDM which was 328 microns. The higher the T_{iso} the more rapid the particle size reduction within 55 °C to 65 °C. It was due to the faster energy influx to BDM crystal and eventually accelerated the rate of solid state transformation and the rate of particle size reduction as the temperature increased. However, for the highest T_{iso} of 70 °C, the dehydration energy of 20 J/g, which effectively reduced the particle size to the smallest at 65 °C, could not successfully decrease the BDM particle size to the range of 30 to 60 microns. When high temperature or energy contacts the outer surface of BDM crystal, BD structure was simultaneously generated on the surface (Amolwan Chinapak, 2000). It would act as the anhydrous barrier and retarded the diffusion rate of water of crystallization remaining inside the BDM crystals. Thus, the rate of dehydration was reduced. However, continuous flow of heat was accumulated

by the internal crystal core and overcome that BD barrier by destroying the remaining hydrate structure synchronously. Consequently, small particle of only anhydrous phase BD was generated after approximately 50 J/g of energy was utilized.

The residual water content of heated BDM was also investigated and is presented in Figure 3.6. Remaining water content was decreased as a function of dehydration time or energy used. In the temperature range of 55 °C to 65 °C, the remaining water continuously reduced with nearly straight line as dehydration energy increased. On the other hand, the water content of BDM when heated at 70 °C (up to approximately 48 J/g) slowly decreased compared to that of other lower T_{iso} and at later stage showed a rapid loss of water (between 48 to 58 J/g). This result correlated with the data which obtained for the particle size reduction (Figure 3.5). At initial stage when BDM was heated at 70 °C, slow rate of dehydration happened due to the anhydrous barrier of BD and also resulted in a slower particle size reduction rate.

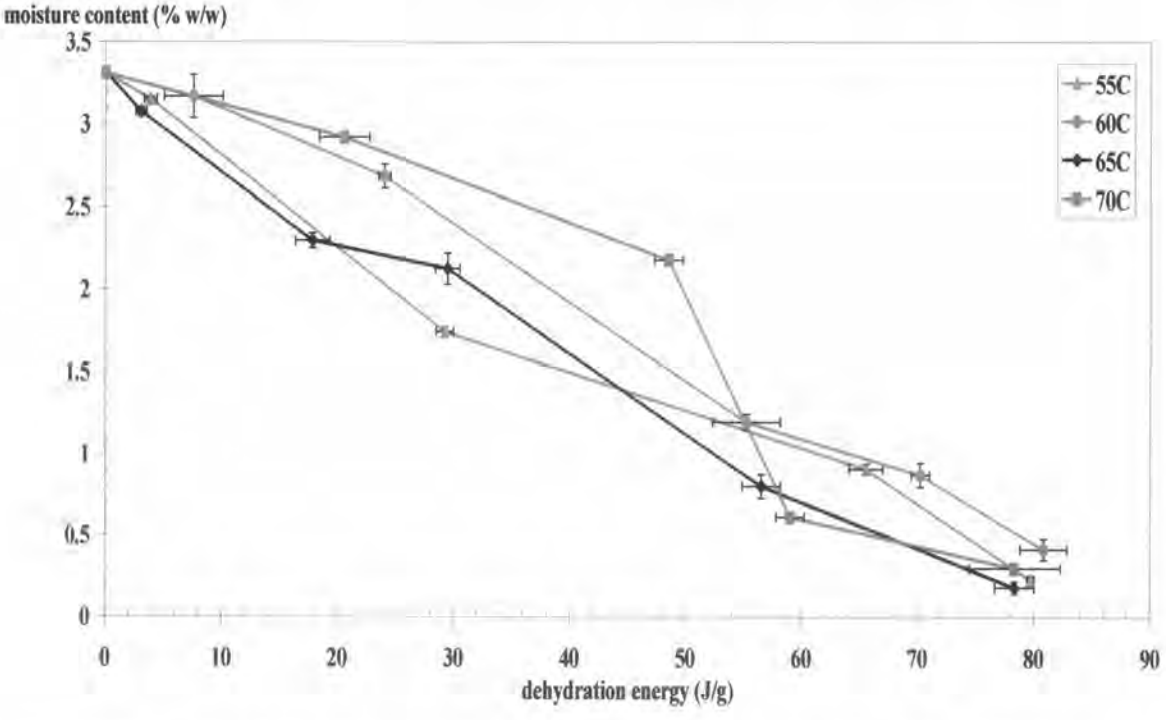

Figure 3.6 The relationship between remaining water content and the dehydration energy when BDM was isothermally heated (T_{iso}) at ▲ 55°C, ● 60°C, ◆ 65°C and ■ 70°C)

A decrease in particle size during dehydration of BDM seemed to have a complex mechanism. The observation of the remaining water was an indirect

indicator to show a transformation between BDM to BD as a function of energy used during heating. Investigation on the actual solid state transformation between BDM to BD was performed by XRPD (Figure 3.7). In this experiment, isothermally heating BDM at 55 °C was investigated. The characteristic peaks of BD and BDM were 8.20, 8.48, 12.64, 13.20, 13.52, 18.78, 19.04, 33.80 °2θ and 9.58, 14.54, 15.58, 18.56, 20.18 °2θ, respectively. At the early stage of dehydration at 10 and 20 mins, which were equivalent to 5 and 30 J/g of energy used, the mix character of BDM and BD were found. Moreover at this point of the 5 and 30 J/g of energy, the remaining water contents were approximately 3 and 1.7 %w/w, respectively. It indicated that BDM still existed in this material due to large amount of residual water content and the mixed pattern in XRPD. However, at 30 J/g the particle size was already reduced to a minimum limit. The particle size reduction occurred prior to complete dehydration and indicated that the powder obtained at the early stage had significant water content inside. After that, more energy was applied by heating BDM and resulted in less remaining water content (less than 1%). In addition, XRPD pattern clearly showed only BD phase at 32 and 55 mins of heating. It could be concluded that the energy consumed at the early stage was mainly utilized to dehydrate which eventually perturbed the structure of BDM and disrupted the particles of BDM. The further thermal energy at the later stage of dehydration was principally consumed to generate pure phase of BD with already existing smallest particle size.

From the above results, it was surprising that the small particles of BDM at certain heating time contained a considerable amount of water. Thus, to better understand this complex phenomenon, SEM of isothermally heated BDM at 55 °C was also investigated (Figure 3.8). SEM photomicrographs showed that at 10 mins of heating, large particles of BDM showed trace of small particle formation on the outer surface of BDM crystals. Hence, early stage of isothermal dehydration showed marked impact on the particle size of BDM. Additional dehydration subsequently changed the solid structure of final small particles with unadulterated anhydrous phase of BD. The particle size distribution of heated BDM showed the gradual dynamic particle size reduction behavior during isothermal dehydration (Figures 3.9-3.12).

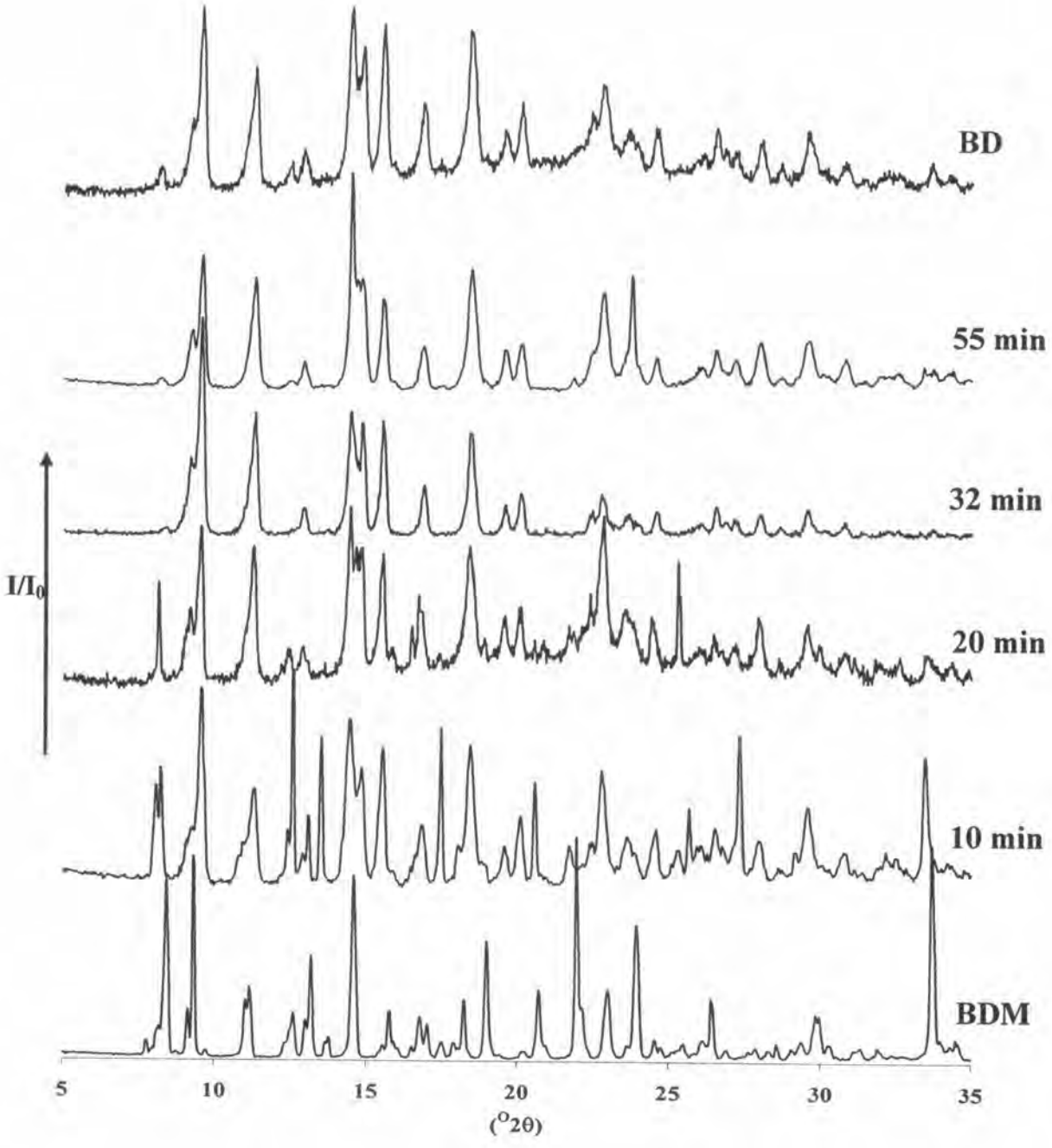

Figure 3.7 XRPD diffractograms of BDM after isothermally heated at 55 °C at different t_{iso}

The particle size distribution of intact BDM was shown to be monodispersed with a mean particle diameter of 328 microns. During the early stage of isothermal dehydration, the particle size distribution became bimodal with the slight shift of the

large particle size to the left and the increase of smaller particle size range (30 to 60 microns). The large particles of heated BDM completely disappeared and turned to the smaller particle size when more energy was applied. The monodispersed character of the smaller particle size appeared at the end stage of isothermal dehydration with minute amount of fines which could be seen by SEM (Figure 3.8).

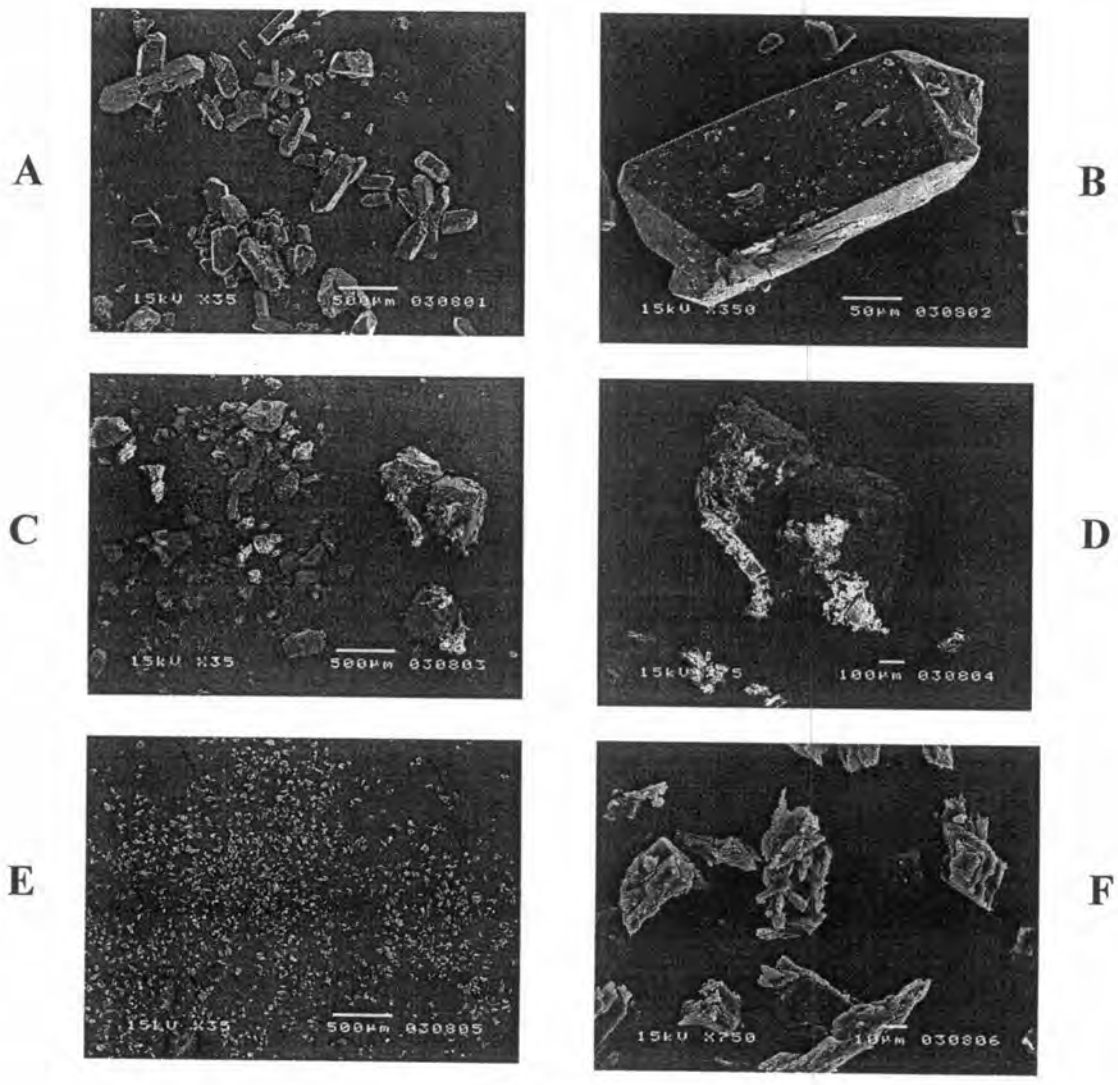

Figure 3.8 SEM photomicrographs of isothermally heated BDM at 55 °C with different t_{iso} (A and B - initial particles at magnification of 35 and 350, C and D - after 10 mins of heating at magnification of 35 and 350, E and F - after 20 mins of heating at magnification of 35 and 750)

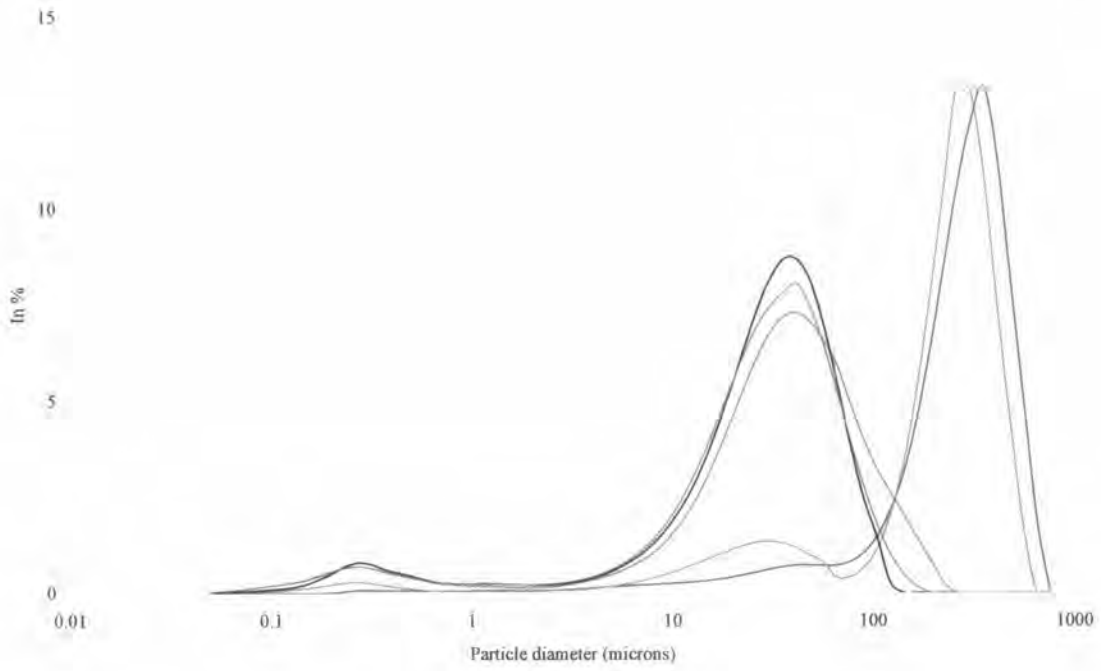

Figure 3.9 The particle size and size distribution of isothermally heated BDM at 55 °C with different t_{iso} (blue line- initial particle, pink line - 10 mins, red line- 20 mins, black line - 32 mins and green line - 55 mins)

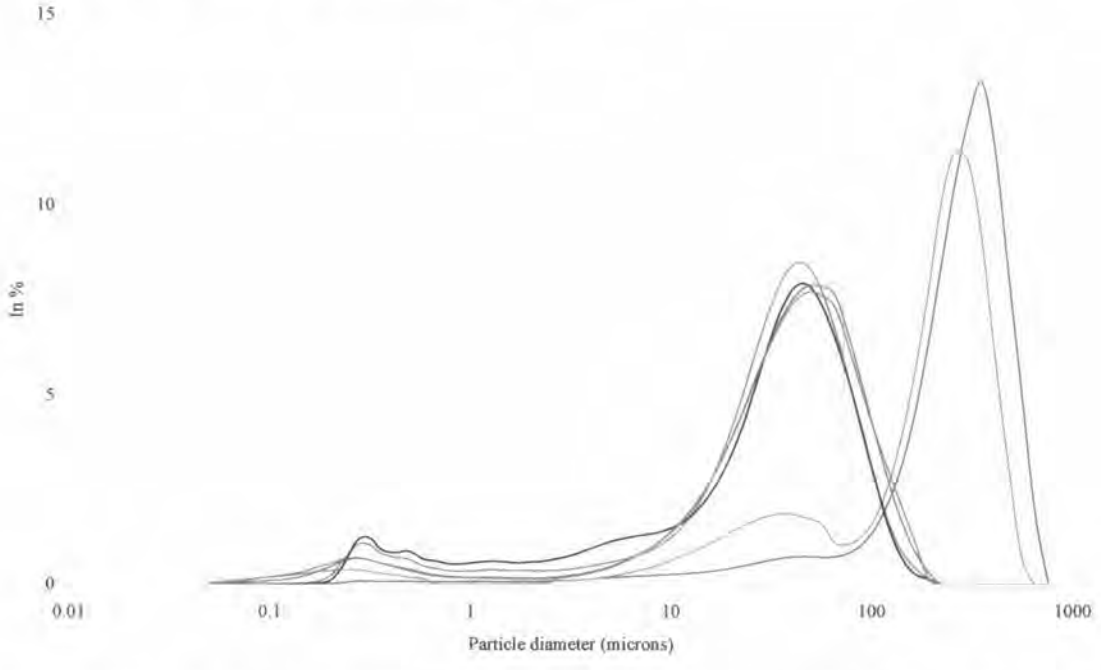

Figure 3.10 The particle size and size distribution of isothermally heated BDM at 60 °C with different t_{iso} (blue line- initial particle, pink line - 10 mins, red line- 15 mins, black line - 20 mins, green line - 28 mins and violet line - 42 mins)

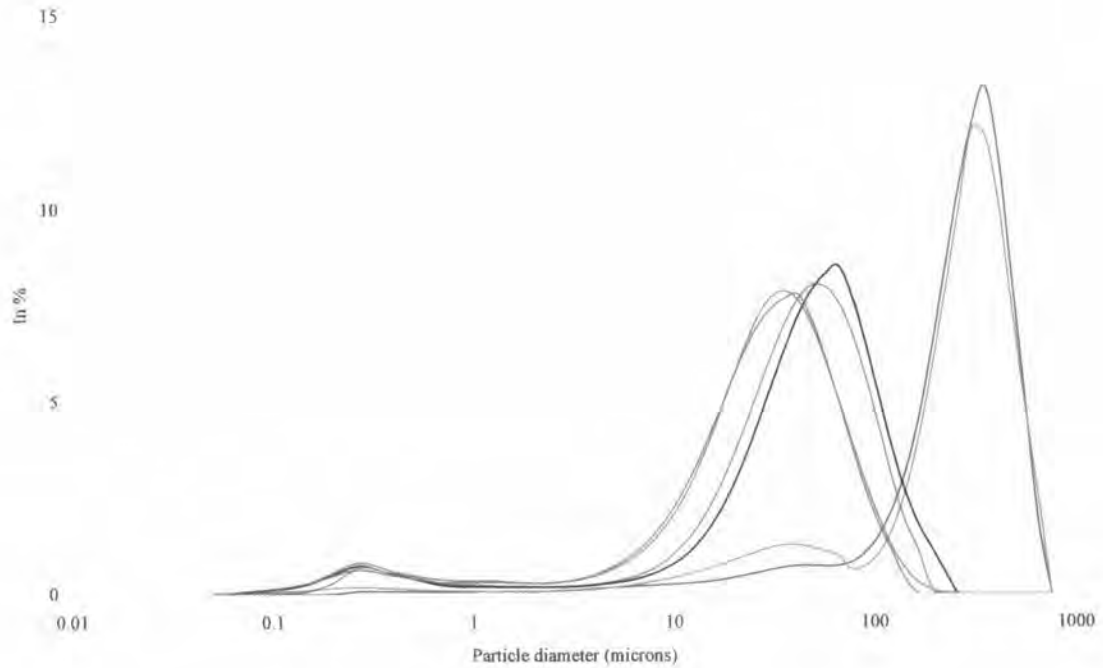

Figure 3.11 The particle size and size distribution of isothermally heated BDM at 65 °C with different t_{iso} (blue line- initial particle, pink line - 5 mins, red line- 7.5 mins, black line - 10 mins, green line - 15 mins and violet line - 27 mins)

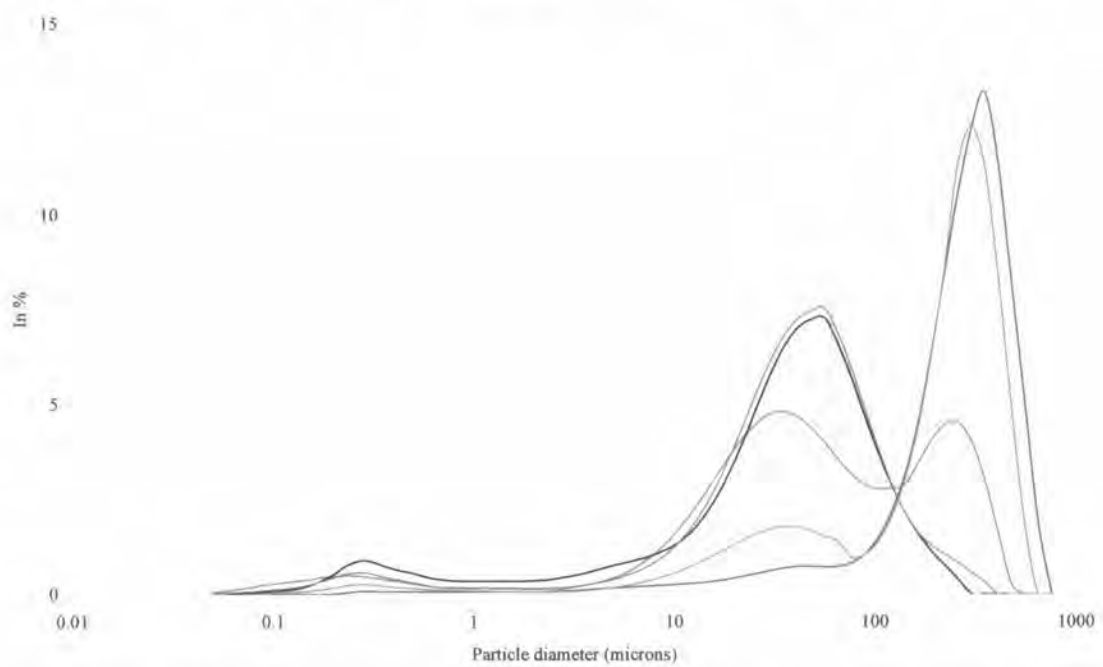

Figure 3.12 The particle size and size distribution of isothermally heated BDM at 70 °C with different t_{iso} (blue line- initial particle, pink line - 3 mins, red line- 5 mins, black line - 8 mins and green line - 22 mins)

Determination of E_a for dehydration of BDM

The dehydration energy for BDM which resulted in smaller particle size of BD was directly determined from AUC obtained from IDSC experiment. On the other hand, the activation energy for dehydration can also be obtained from the calculation from either model dependent solid state kinetic or model independent solid state kinetic.

E_a theoretically means "a physicochemical quantity that represents the barrier for a chemical reaction" (Byrn et al., 1999 and Laidler, 1984). According to the method for calculation of E_a, fraction reacted (α) and dehydration time (t) at different T_{iso} were identified (Figure 3.13). This relationship of the dehydration of BDM at every T_{iso} demonstrated an induction phase of reaction shown by an early constant period of α. It was suggested that dehydration of BDM needed a sufficient energy at the initial stage to activate the dehydration process. The second phase of gradually increasing dehydration as a function of t for all α-t curves were present after the induction period. The third late constant phase of every α-t curves were illustrated which the end period of reaction were well defined. In addition, the water content of heated BDM at final period was analyzed and found to be very low. It also confirmed that the final phase of dehydration resulted in the generation of the anhydrous phase.

Regarding the model dependent solid state kinetic approach, the transformation of all α–t data at every T_{iso} were fitted with definite solid state kinetic equations (see Appendix C). Several kinetic equations usually gave good fit with solid state kinetic data. The results suggested that the data could fit with many kinetic equations with a high level of correlation (r^2 more than 0.99). The correlation of natural logarithm of rate constant (ln k) obtained from several kinetic equations and 1/T were established and are shown in Figure 3.14. The E_a in which were evaluated from the slope of above relationships are tabulated in Table 3.2. Activation energies for dehydration of BDM derived by calculating from various equations were consistent within the range of 70 to 83 kJ/mol.

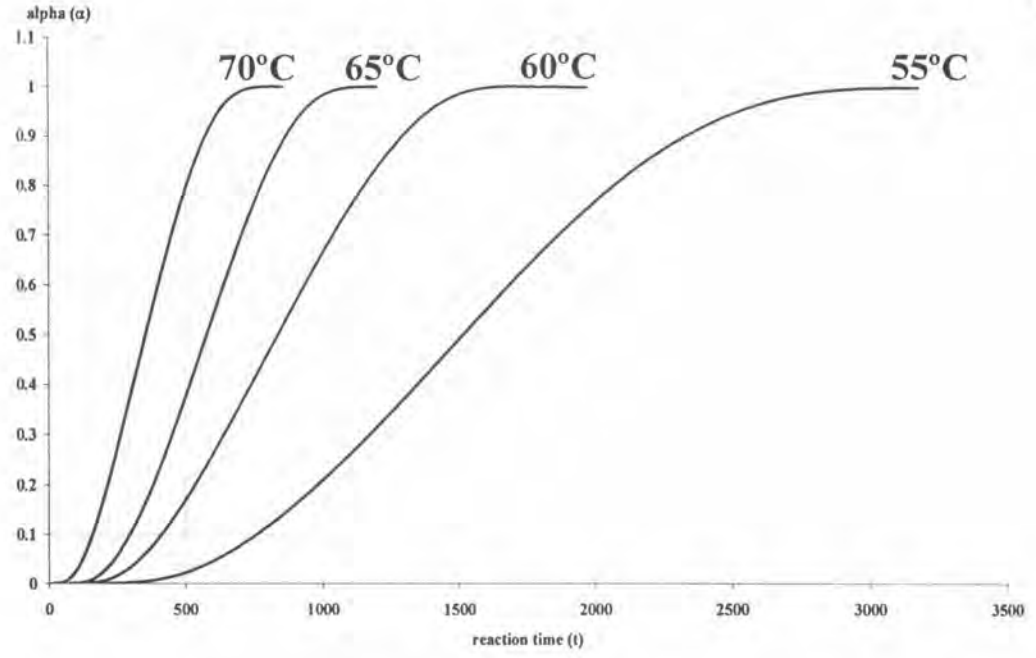

Figure 3.13 The α–t curves of BDM dehydration at different T_{iso} obtained by IDSC experiments

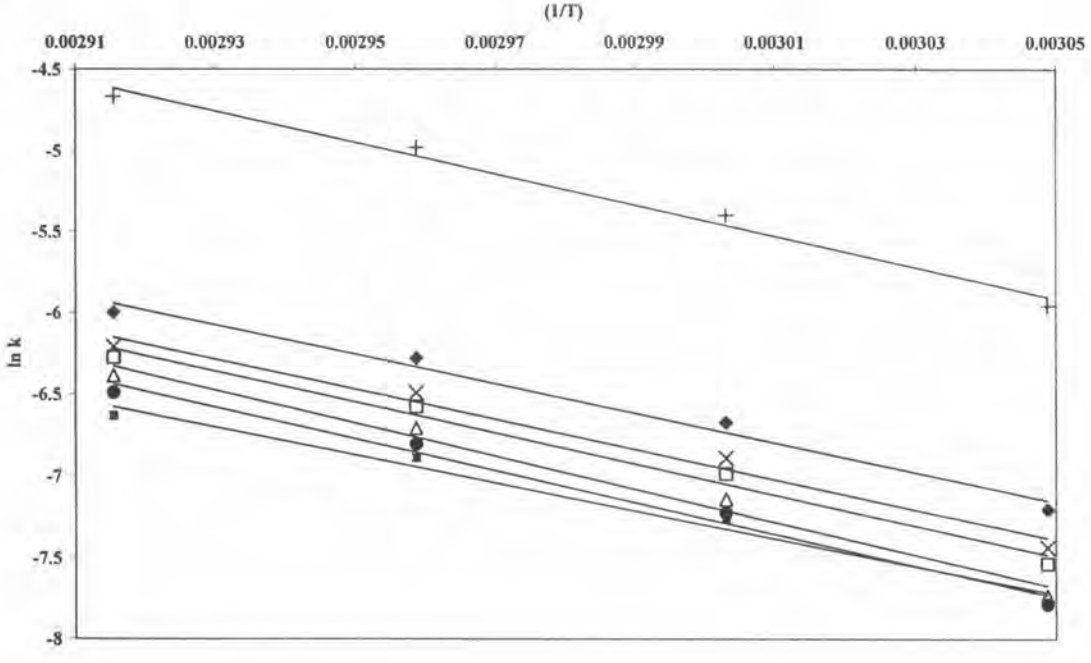

Figure 3.14 The relationship between ln of rate constant (ln k) and the reciprocal of absolute temperature (1/T) of model dependent approach of dehydration kinetic of BDM (+ Prout-Tompkins model, ◆ 1 dimensional Avrami Eroféev model, □ 2 dimensional Avrami Eroféev model, • 3 dimensional Avrami Eroféev model, × 1 dimensional Phase Boundary model, ■ 2 dimensional Phase Boundary model and △ Power Law (n=1/2) model)

Table 3.2 The E_a of isothermal dehydration of BDM with various solid state kinetic models

Model equation	E_a (kJ/mol)
Avrami Erofeev	
• 1 dimensional	74.87
• 2 dimensional	78.37
• 3 dimensional	80.49
Power Law	
• n = 1/2	83.52
Phase Boundary	
• 1 dimensional	76.20
• 2 dimensional	70.82
Prout-Tompkins	80.40

The dehydration of BDM followed Avrami Erofeev equations with one, two and three dimensional. Thus, the mechanism of dehydration might due to the random nuclei generated along one, two or three dimensions and progressively ingested other nuclei. In addition, Prout-tompkins model also correlated, indicated the mechanism of dehydration was controlled by linearly forming of nuclei and grows as a chain reaction. However, phase boundaries model showed good agreement with the dehydration of BDM. This result showed that the advancement of dehydrated phase from the outside of particle was the main mechanism during dehydration. However, the actual mechanism of dehydration of BDM composed of several mechanism which seen from the formation of small particles of dehydrated phase and followed with the solid state dehydration. Therefore, there was not only one solid state kinetic models could not totally described the complex dehydration mechanism of BDM.

Due to the disadvantage of model dependent approach which assumed the E_a is constant throughout the reaction, model independent or model free kinetic is recently redeveloped and employed (Vyazovkin, 2000; Zhou et al., 2003). The E_a from model independent approach were in the range of 80 to 87 kJ/mol which was similar to that from model dependent approach (Figure 3.15). The results showed that the thermal energy of 80 to 90 kJ was needed to drive the dehydration reaction of one mole BDM. Dehydration reaction rate of BDM was temperature dependent reaction.

The higher the dehydration temperature the faster the rate of dehydration. In addition, the E_a continuously and slightly decreased when α gradually increased. It was assumed to be due to the change in particle size of BDM during dehydration. The surface area of small particles of BDM normally higher than intact BDM and provided numerous sites for dehydration. In addition, the surface area over volume ratio was also altered and reduced the energy barrier of dehydration. The E_a of dehydration could be employed to indicate an ease of the generation of dehydration reaction.

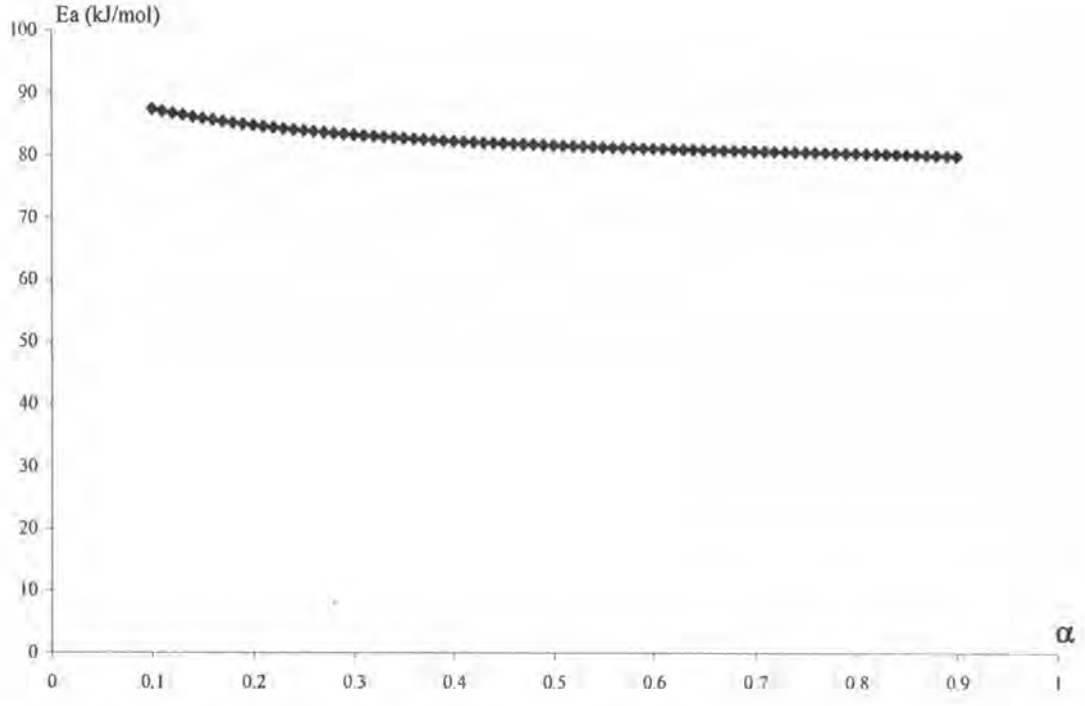

Figure 3.15 The E_a-α curve of model independent approach for isothermal dehydration of BDM

The escape of crystallizating solvent out of the solvate is influenced by several factors (Byrn et al., 1999). One of the most important is crystallographic direction that offers the least resistance to the movement of solvent molecules. Other crystal packing parameters also play a pivotal role on the limitation of the escaping of solvent away from its host structure. The larger the tunnel size, by approximately measuring the cross sectional area of the tunnel, the easier the loss of solvent from the solvate structure. In addition, the number of tunnel per unit area, tunnel shape, tortuosity and the arrangement of solvent molecules along the channel are of great concern. The zig-

zag shape of tunnel will hinder the exit of solvent. The more tunnel per unit area, the greater the ease of solvent escaping. The compactness of the crystal packing is demonstrated by crystallographic parameters. The increase in molecular volume after solvate formation from ansolvate will tell us about the compactness of crystal packing. The more loosely packed the less obstacle for solvent loss. Other parameters which become increasingly important are the type and number of hydrogen bonding between solvent and the active moiety in the solvate. Obviously, in order to exit the host structure, it is necessary to brake down the attachment force between solvent and host. Thus, the higher number of bonding and the stronger bonding will need more energy to destroy the solvent bonding from the solvate.

Table 3.3 Crystallographic data of BD and BDM from single crystal X-ray diffraction (SC-XRD)

Crystal data	BDM[a]	BD[b]
Empirical formula	$C_{28}H_{39}ClO_8$	$C_{28}H_{37}ClO_7$
Molecular weight	539.06	521.03
Space group	Orthorhombic	Orthorhombic
	$P2_12_12_1$	$P2_12_12_1$
***a* (Å)**	14.1520	12.1239
***b* (Å)**	16.2680	14.1289
***c* (Å)**	12.0849	14.8381
crystal volume (V, Å^3)	2782.2	2541.7
Z	4	4
Density (Dx, mg.m^{-3})	1.290	1.362

[a] Duax, Cody and Strong, 1981

[b] Millard and Myrdal, 2002

Calculation of K channel (K_{chan}) (Perlovich et al., 1996 and 1998)

The concept of K_{chan} was adapted to determine the compactness of solvent packing in the lattice channel. The higher K_{chan} suggest a more compact crystal packing in definition. The calculation of K_{chan} was derived from the following equation

$$K_{chan} = \frac{Z \cdot n \cdot V(solvent)}{[V(solvate) - V(ansolvate)]} \quad \ldots(23)$$

Where Z is the number of active molecule per unit cell, n is the stoichiometry of solvate, V(solvent) is the molecular volume of entrapped solvent in the solvate form, V(solvate) is unit cell volume of the solvate form and V(ansolvate) is the unit cell volume of form without entrapped solvent.

From crystallographic data of BD and BDM (Table 3.3), K_{chan} was calculated. Monohydrate form of BD (BDM) showed the n value of 1 and Z is 4. In addition, the molecular volume of water or entrapped solvent in BDM is approximately 10 $Å^3$ (Chakarvarty, Bhinge and Varadarajan, 2002). The difference in unit cell volume of the anhydrous form and the monohydrate form was determined and found to be equivalent to 240.5 $Å^3$. All of above values resulted in the K_{chan} of 0.1663. Due to a lower K_{chan} of 0.1663 indicating less compactness of crystal packing, it directly meant that water of crystallization in BDM structure occupied the space or volume in crystal lattice of less than 16%. There was high free volume (up to 84%) to allow water for more molecular mobility. The water of crystallization molecules could have more opportunity to move themselves out of lattice after certain energy was introduced into their structures. This low K_{chan} agreed well with K_{chan} derived from the calculation of the raw data obtained from Redman-Furey et al. (2005) and Lester et al. (2006) of risedronate sodium hemihydrate.

Crystallographic data of BDM from the SC-XRD analysis provides information concerning the molecular interaction between one water of crystallization with two adjacent BD molecules in the crystal lattice unit (Figure 3.16). With the aid of Mercury® software, the hydrogen bonds and their properties which occurred between water molecules and BD moeities were determine and are summarized in Table 3.5. Firstly, the position of each atom of each species was defined for their three dimensional position (Figure 3.17). The oxygen atom of water molecule was assigned as O8 and the two attached hydrogen atoms were assigned H38 and H39, respectively. Meanwhile, BD molecules were also assigned the atomic positions as can be seen in Figure 3.17. The most important atoms for hydrogen bonding in BD are O6 and O7 including O2 that already coupled with H37. There were three important hydrogen bonding positions in the lattice unit (Figure 3.18). Two out of three hydrogen bonds were directly formed via the interactions of H38 and H39 of the water molecules to

O7 and O6 of BD, respectively. The remaining hydrogen bond at H37 of BD interacted with O8 of water molecule. The interactions at H38-O7 and H39-O6 were generally presented as O7-H38-O8 and O6-H39-O8 according to the common nomenclature for hydrogen bonding. The H37-O8 bond was also rewritten as O2-H37-O8.

Table 3.4 The properties of strong, moderate, and weak hydrogen bonds (Jeffrey, 1997)

	strong	**moderate**	**weak**
A-H----B interaction*	mostly covalent	mostly electrostatic	electrostatic
Bond lengths	A-H ≈ H----B	A-H < H----B	A-H << H----B
H----B (Å)	~ 1.2-1.5	~ 1.5-2.2	~ 2.3-3.2
A----B (Å)	2.2-2.5	2.5-3.2	3.2-4.0
Bond angles (°)	175-180	130-180	90-150
Bond energy (kcal/mol)	14-40	4-15	<4

* A is hydrogen donor and B is hydrogen acceptor

Theoretically, the longer the bond length the lower the bond energy. Therefore, the longer bond length of hydrogen bond is defined as the weaker bond with lower bond energy as seen in Table 3.4. The properties of each hydrogen bond in BDM structure clearly showed the moderate to weak hydrogen bond type as determined by Mercury® software (Table 3.5). Bond length and bond angle between hydrogen donor to acceptor or A----B position of all hydrogen bonds in BDM fell into the moderate hydrogen bond type. However, the other important value and must also take into account was the length between H----B position. The H----B bond length of O2-H37-O8 equals to 2.140 that classified as moderate hydrogen bond type. Another value of H----B of O6-H39-O8 and O7-H38-O8 were 2.227 and 2.431, respectively. They could be categorized as weak type hydrogen bonding. Although all of the hydrogen bonds were the moderate type according to A----B aspect but the H----B aspects indicated one moderate plus two weak hydrogen bonds. It was suggested that BDM has moderate to weak type hydrogen bonding.

Table 3.5 The hydrogen bond positions and molecular property of BDM crystal structure from crystallographic data

Bond definition	Hydrogen bond position	Bond length (Å)	Bond angle(°)	Type of hydrogen bond
	O2-H37-O8			
A----B	O2-O8	2.770	176.48	Moderate
H-A	O2-H37	0.631		
H----B	H37-O8	2.140		
	O6-H39-O8			
A----B	O6-O8	2.881	149.42	Moderate to
H-A	H39-O8	0.706		Weak
H----B	O6-H39	2.227		
	O7-H38-O8			
A----B	O7-O8	2.918	144.35	Moderate to
H-A	H38-O8	0.575		Weak
H----B	O7-H38	2.431		

The interaction between water of crystallization itself was focused. The arrangement of water molecules in BDM exhibited a tunnel like hydrate along *a* axis (Figure 3.19) while it could not be seen through the *b* and *c* axis. It was said that BDM is a channel hydrate. Normally, channel hydrate easily looses their water of crystallization through a tunnel when the end of the lattice unit is open. In this situation, there was only one possible way for water removal on either ends of the *a* axis.

The data of K_{chan}, hydrogen bond and the arrangement of water of crystallization in tunnel of BDM suggested the ease of water of crystallization removal. All of above details were the crystallographic aspects explaining the complexity of thermal dehydration of BDM resulting in final particle size reduction

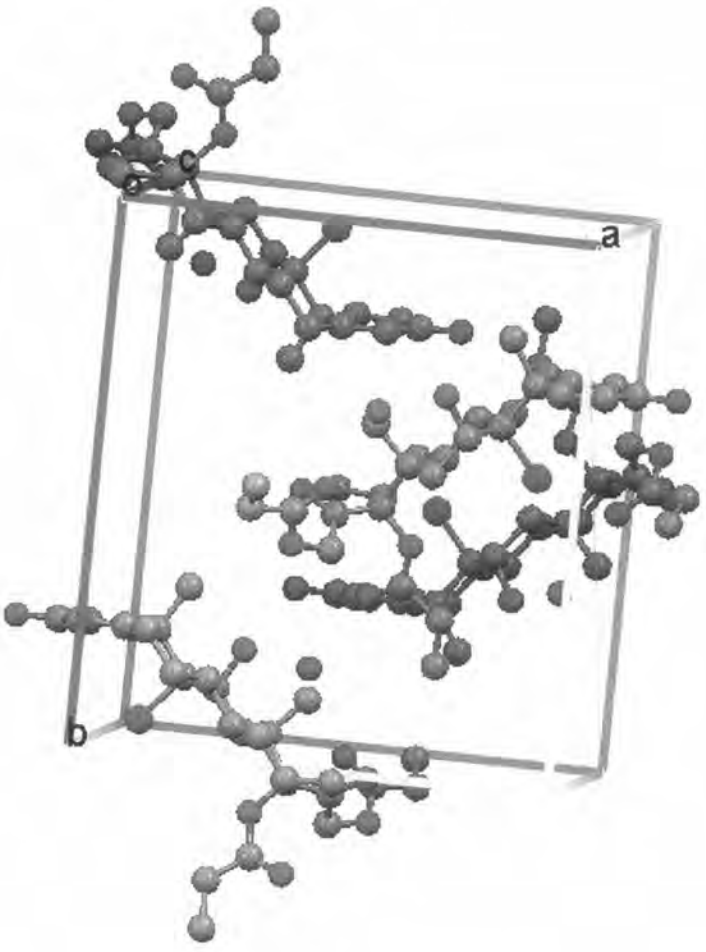

Figure 3.16 The crystal packing of BDM (free red dots are represent water molecules) as obtained by Mercury® from the Cambridge Structural Database (CSD) code: BCLMSN.

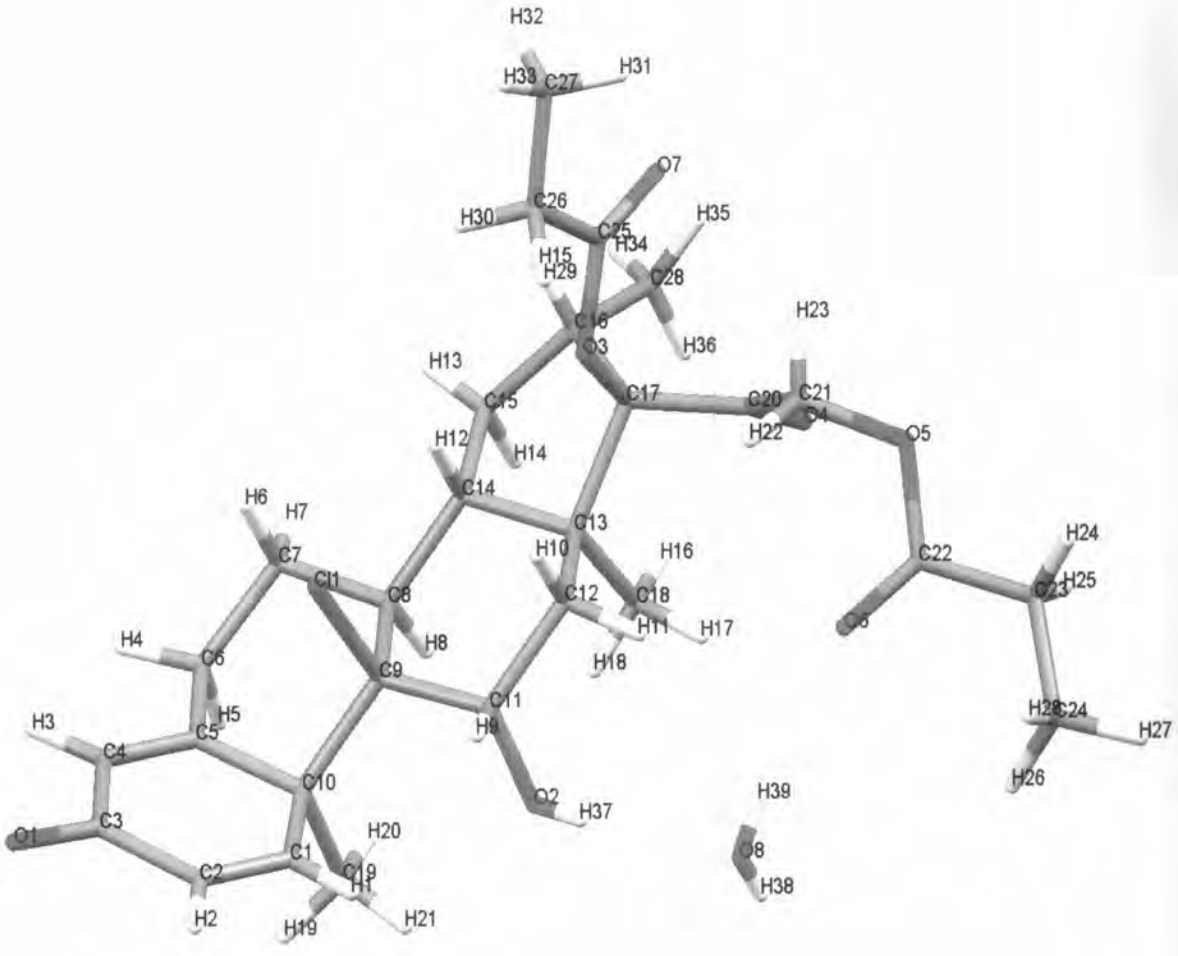

Figure 3.17 The atomic positions of BDM in three dimensional

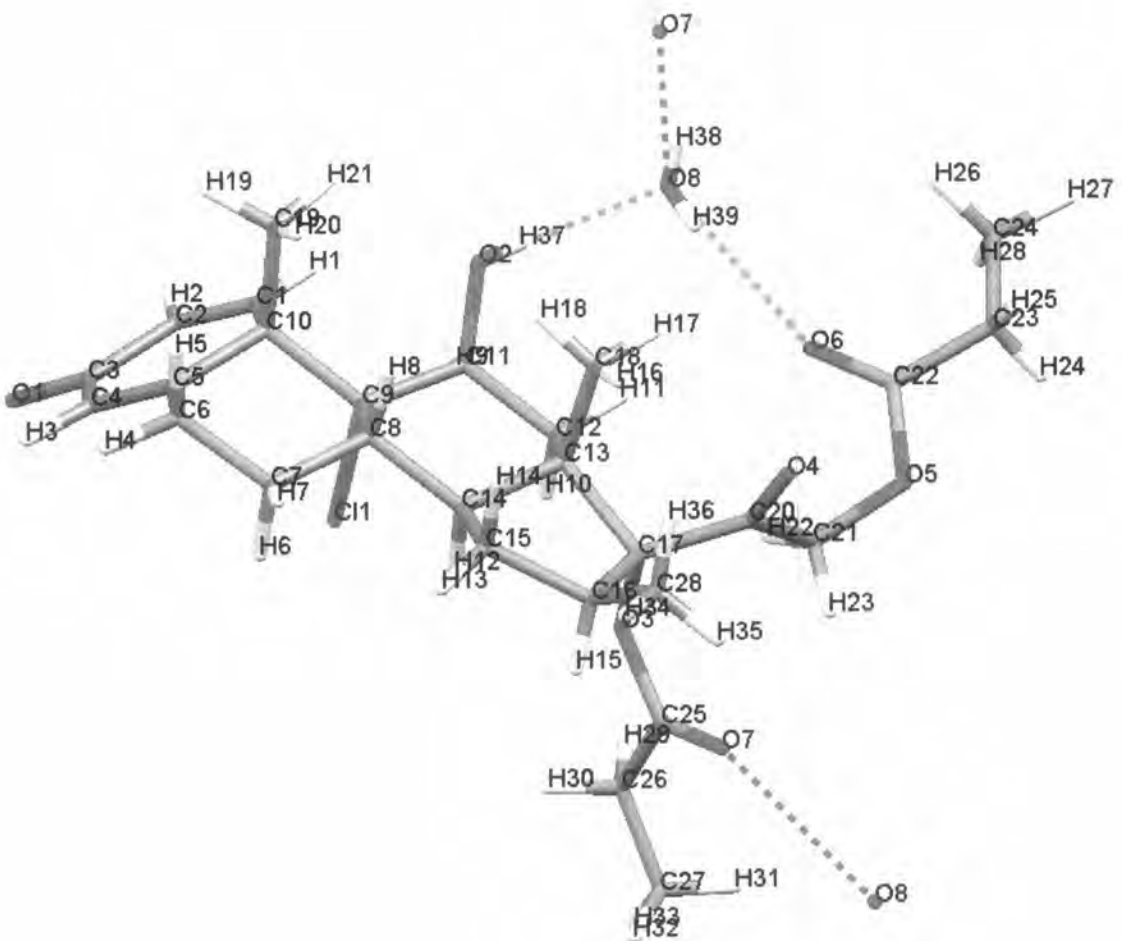

Figure 3.18 The hydrogen bonding between water molecule and BD moiety in BDM

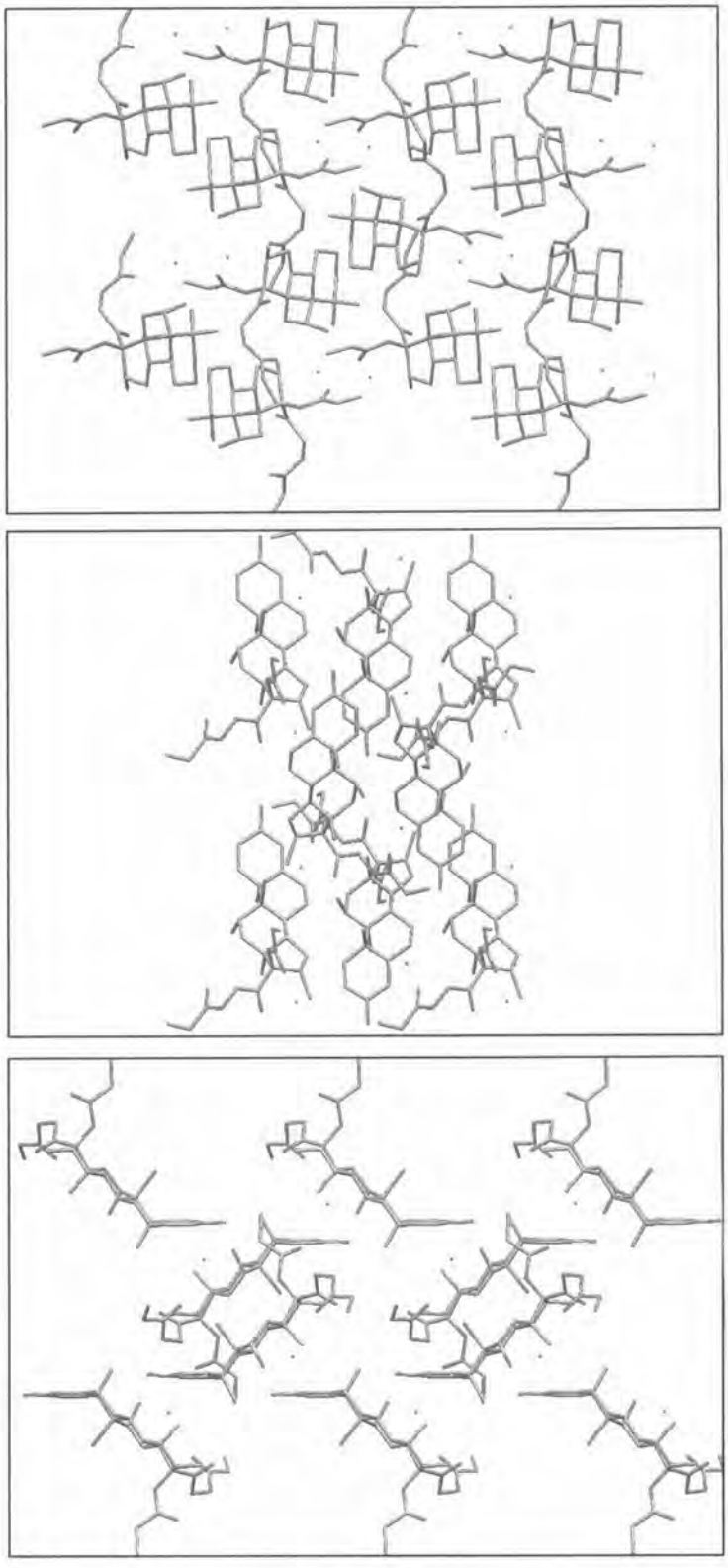

Figure 3.19 The crystal packing of BDM along different axis (free red dots are represent water molecules)

3.4 CONCLUSIONS

Particle size reduction of BDM by thermal dehydration had been demonstrated (Amolwan Chinapak, 2001). In this study, thermomicroscopic method clearly confirmed the dehydration induced particle size reduction phenomena of BDM. The change in BDM during drying indicated the disruption of crystal BDM and led to a smaller particle size of BD. Initial step of dehydration of BDM showed the transformation of BDM to BD from outer surface and progressed to the inner core of the BDM crystal. The BD particles surrounding BDM are very small and irregular in shape. The particle size reduction of BDM was completed before total dehydration of BDM occurred. In addition, the solid structural transformation of BDM to smaller particles of BD was incomplete even when the size of the solid was reduced to the lowest. Hence, the size of BDM was decreased at the initial step of dehydration and after that the loss of water continuously happened and eventually yields the smallest size of BD at the later step of dehydration.

The thermal dehydration of BDM was complex since it composed of particle size reduction and dehydration at the same time. The particle size reduction phenomenon occurred prior to a complete dehydration with the apparent energy for particle size reduction lower than the energy for the complete dehydration process. The apparent particle size reduction energy highly depend on the level of drying temperature, that is, the higher the drying temperature, the lower the apparent particle size reduction energy. In the case of very high drying temperature, the apparent particle size reduction energy was higher than that of lower temperatures used. It was due to the fact that anhydrous BD barrier formed around the outer surface of BDM. Thus, the removal rate of water was retarded and the change in their crystallographic property was reduced.

The total energy required for complete dehydration did not depend on the drying temperature as shown by the same calculated total dehydration energy. However, IDSC studies showed that the "rate" of dehydration highly depend on the level of temperatures used. A study on evaluating activation energies was done to confirm this finding. It was shown that the calculated activation energy derived from both model dependent and model independent solid state kinetics were in the same range and provided a positive value. It indicated that the dehydration "rate" of BDM

was the temperature dependent. The higher the drying temperature the faster the "rate" of dehydration confirming the results obtained from IDSC studies.

On the crystallographic point of view, the packing and bonding between BD molecules and water of crystallization in the same crystal lattice unit played a major role on the unique dehydration process. Due to the low coefficient of packing (K_{chan}), 0.1663, it was easy to loose water molecules from the crystal lattice. Additionally, the major force for attachment of water with BD was dominantly through hydrogen bonding. All of the hydrogen bonds in BDM were identified as moderate to weak type hydrogen bonding. It could be implied that less energy could overcome such binding forces and directly impacted on the new arrangement of anhydrous phase of BDM. Since the low of the coefficient of packing and the weak hydrogen bonding, the water of crystallization in BDM could be removed easily with small amount of energy. The loss of water of crystallization from BDM crystal lattice led to generate an imperfection of the internal structure. The lower structural integrity would induce a weak physical property of the solid particles. Therefore, the structural collapse of BD happened after BDM was partially dehydrated; hence, the small particle of BD was later obtained.

In conclusion, the complex dehydration behavior of BDM is a good model to show the change in crystal size with partial solid state transformation to the anhydrous phase at the early stage of dehydration followed by the complete dehydration with complete transformation to anhydrous BD. From this study, it is possible to employ dehydration to other solvated structure to generate anhydrous form with smaller particle size. In order for this phenomena happen, the interested solvate must have low K_{chan} and looses water easily, if possible, through tunnels or channels leaving a very fragile structure. The solid structure will then collapse, the particle size will be reduced and the energies involved may be calculated. However, further study must be performed to evaluate the specific structure of active pharmaceutical ingredients for this "dehydration induced particle size reduction" to occur.